Published in final edited form as:
Nanomedicine. 2012 April ; 8(3): 291–298. doi:10.1016/j.nano.2011.06.012.

Protective Effect of the Apoptosis-Sensing Nanoparticle AnxCLIO-Cy5.5

Howard H. Chen, PhD[1,2], **Yan Feng, MD**[3], **Ming Zhang, MD**[3], **Wei Chao, MD PhD**[3], **Lee Josephson, MD PhD**[2,5], **Stanley Y. Shaw, MD PhD**[1,4], and **David E. Sosnovik, MD**[1,2]

[1]Center for Molecular Imaging Research, Massachusetts General Hospital, Harvard Medical School

[2]Martinos Center for Biomedical Imaging, Massachusetts General Hospital, Harvard Medical School

[3]Department of Anesthesia and Critical Care, Massachusetts General Hospital, Harvard Medical School

[4]Center for Systems Biology, Massachusetts General Hospital, Harvard Medical School

[5]Center for Translational Nuclear Medicine and Molecular Imaging, Massachusetts General Hospital, Harvard Medical School

Abstract

The diagnostic utility of the apoptosis sensing nanoparticle, AnxCLIO-Cy5.5, is well established. Here we sought to define the pathophysiological impact of the nanoparticle on apoptotic cells. Confocal microscopy showed that AnxCLIO-Cy5.5 remained bound to apoptotic cell membranes for 3 hours, but by 7 hours had become completely internalized. AnxCLIO-Cy5.5 exposure did not impact energetics, metabolism or caspase-3 activity in apoptotic cells. Gene expression in cells exposed to AnxCLIO-Cy5.5 did not reveal upregulation of pro-inflammatory or cell death pathways. Moreover, exposure to AnxCLIO-Cy5.5 decreased the frequency of membrane rupture of early apoptotic cells. Similarly, in mice exposed to 1 hour of ischemia-reperfusion, the injection of AnxCLIO-Cy5.5 at the onset of reperfusion reduced infarct size/area-at-risk by 16.2%. Our findings suggest that AnxCLIO-Cy5.5 may protect apoptotic cells by stabilizing their cell membranes and has the potential to become a theranostic agent, capable of both identifying and salvaging early apoptotic cells.

Keywords

Apoptosis; Magnetic Nanoparticle; Cardioprotection; Iron Oxide; Gene Expression

Corresponding author, David E. Sosnovik, MD, CNY, Massachusetts General Hospital, 149 13th Street, Charlestown, MA 02129, USA., Tel: 617 724 3407; sosnovik@nmr.mgh.harvard.edu.

Conflict-of-Interest: None

Background

Apoptosis plays a central role in diseases such as ischemia-reperfusion and heart failure.[1, 2] However, despite major progress in elucidating the molecular mechanisms of apoptosis, the translation of this knowledge into new therapeutic strategies has been slow. Techniques to image apoptosis in vivo have thus been developed to attempt to bridge the gap between basic science and clinical translation.[3] Most of these techniques have used the ligand Annexin V (Anx) to bind to the outer surface of apoptotic cells.[4] Validation of this approach was initially performed in small animals with fluorescent annexins, and subsequently in humans with ^{99}Tc-Anx.[5–7] More recently, annexin-labeled nanoparticles, such as AnxCLIO-Cy5.5, have been developed and used to image apoptosis in the heart in vivo.[8, 9]

The AnxCLIO-Cy5.5 nanoparticle, developed in our group, consists of Annexin V (Anx) conjugated to the magnetofluorescent nanoparticle CLIO-Cy5.5 (CLIO=cross-linked iron oxide). The diagnostic utility and accuracy of AnxCLIO-Cy5.5 has been shown in both ischemic heart disease and heart failure.[10, 11] Fluorescence microscopy in these studies showed that the agent binds to the outer surface of apoptotic cardiomyocytes, while their cell membranes are still intact. While this allows apoptotic cells to be imaged in vivo, the impact of AnxCLIO-Cy5.5 on the apoptotic cell remains unknown. The purpose of this study was thus to characterize the effects of AnxCLIO-Cy5.5 on early apoptotic cells, and to determine whether the use of AnxCLIO-Cy5.5 would facilitate their salvage or accelerate their demise.

The impact of AnxCLIO-Cy5.5 was tested in several cell lines in vitro, and in a mouse model of myocardial ischemia-reperfusion in vivo. Metrics such as cell viability, membrane integrity, ATP content, mitochondrial membrane potential and reducing capacity were measured.[12] The impact of the nanoparticle on infarct size and left ventricular function was tested in vivo. In addition, gene expression analysis was performed to assess the impact of AnxCLIO-Cy5.5 on cell metabolism in more detail. The results of our study show that AnxCLIO-Cy5.5 is extremely well tolerated by apoptotic cells and that uptake of the agent does not adversely affect apoptotic cells. In fact, our data suggest that AnxCLIO-Cy5.5 may exert a mildly protective effect both in vitro and in vivo. This is consistent with a growing body of literature suggesting that certain formulations of annexin may have a therapeutic and protective role.[13, 14] The results of this study thus suggest that AnxCLIO-Cy5.5 may be of significant utility, not only as a diagnostic nanoparticle, but also as a vehicle for cell protection and the delivery of novel therapeutics.

Methods

In Vitro Studies

Apoptosis was induced in three cell lines (CHO, 786-0 and H9C2) by exposure to either 1 or 5μM of camptothecin (Sigma, St Louis, MO) for 6–24 hours. The cells were collected, pelleted in glass test tubes, and then resuspended in a calcium-containing annexin-binding buffer (Invitrogen, Carlsbad, CA). The presence of apoptosis in the cells was confirmed with flow cytometry (FACS) using Anx-FITC and propidium iodide (PI) (Invitrogen). The fluorescent dyes were added to the cells and incubated for 15 minutes at 37°C, after which time the cells were filtered and kept on ice until FACS. FACS was performed using the 3 Laser LSR II system (Becton-Dickinson, Franklin Lakes, NJ) and the manufacturer suggested filter settings. Each FACS readout was based on 10^4 events, and compensation was done digitally when necessary. The results were analyzed using the Flowjo (Tree Star, Ashland, OR) and Prism (Graphpad, La Jolla, CA) software packages. Cells that were annexin positive and PI negative were labeled as apoptotic, and those that were PI positive as necrotic. Each experimental condition was performed in triplicate and repeated on 3 independent occasions (n=9).

The affinity of AnxCLIO-Cy5.5 for apoptotic cells was tested by co-exposing camptothecin (CPT) treated CHO cells to AnxCLIO-Cy5.5 and Anx-FITC. The proportion of PI negative cells stained with the two agents was compared. The location and trafficking of AnxCLIO-Cy5.5 on apoptotic cells was then studied with time-lapse confocal microscopy using a LSM510 confocal microscope (Zeiss, Oberkochen, Germany). AnxCLIO-Cy5.5 was added to CPT-treated 786-0 cells cultured on a 4-chambered coverglass (Lab-Tek, Rochester, NY). After 15 minutes of incubation at 37°C, the medium was removed and the cells were washed 3 times with phosphate buffered saline (PBS). The cells on the slide were then maintained in medium containing annexin-binding buffer for the duration of the confocal experiment. PI was added directly to the cells immediately before imaging. During imaging, slides containing the cells were enclosed in humidified imaging chamber maintained at 37°C with 5% CO_2.

The effect of AnxCLIO-Cy5.5 on cell energetics and metabolism was tested in CHO cells exposed to 5μM camptothecin for 24 hours. The following assays were used: JC-1 (Invitrogen) for mitochondrial membrane potential, Resazurin (Invitrogen) to measure cell reducing capacity, and CellTiter-Glo (Promega, Madison, WI) to measure cell ATP content. After exposure to 5μM CPT for 24 hours to induce apoptosis, cells were exposed to either AnxCLIO-Cy5.5 (0.325μg Fe/ml) or an equal volume of annexin-binding buffer for 12 hours. The JC-1 and Resazurin reduction assays were quantified using a fluorescence plate reader (Molecular Devices, Sunnyvale, CA). The luminescence readout for the CellTiter-Glo assay was carried out using a custom built bioluminescence imager and quantified in Osirix (freeware, University of Geneva). All assays were carried out in Costar black, clear bottomed 96-well plates (Fisher Scientific, Pittburgh, PA) to avoid signal bleaching into neighboring wells. Each experimental condition was performed in triplicate and repeated on 3 independent occasions (n=9).

The impact of AnxCLIO-Cy5.5 on cell membrane integrity was tested in a rat myocyte line (H9C2), a human epithelial cell (786-0) line, and a hamster ovarian cell line (CHO). Apoptosis was induced in these cells by exposure to 1μM of CPT for 12 hours. The H9C2 and 786-0 cells were then exposed to either AnxCLIO-Cy5.5 (0.325μg Fe/ml) for 1, 4, 7 hours or to annexin-binding buffer only. The CHO cells were exposed four conditions: AnxCLIO-Cy5.5 or binding buffer, as described above, and in addition to either annexin V or CLIO alone for 7 hours. At the end of the exposure period, FACS analysis with PI was performed to determine the number of apoptotic cells that had undergone cell membrane rupture. Caspase-3 activity was also measured in the cell 786-0 lysates using a luminescence-based assay (Promega). Each experimental condition was performed in triplicate and repeated on 3 independent occasions (n=9).

Gene Expression Studies

Whole-genome gene expression studies were carried out with a human epithelial cell line (786-0). The cells were exposed to 1μM of CPT to induce apoptosis and then one half of the cells were exposed to AnxCLIO-Cy5.5 for 7 hours and the other half to annexin-binding buffer only. At the end of the exposure period, cells were sorted with Anx-FITC and PI on a FACSAria cell sorter (Becton-Dickinson) to yield a population of purely apoptotic cells. The cells were flash frozen in liquid nitrogen for gene expression studies. Genome-wide expression data were generated in the Partners HealthCare Center for Personalized Genetic Medicine (PCPGM) microarray facility using standardized protocols. RNA was extracted from the frozen cell pellets of 1.5 million early apoptotic cells with TRIZOL reagent followed by RNeasy column purification (Qiagen, Valencia, CA). The protocol was performed on 3 independent biological replicates for each experimental condition (AnxCLIO-Cy5.5 nanoparticle exposure or buffer only). RNA integrity was assessed with the Agilent 2100 Bioanalyzer platform (Agilent, Santa Clara, CA) prior to hybridization

onto Illumina Human HT-12 v3 DNA microarray chips (Illumina, San Diego, CA). The chips were read on an Illumina Beadstation scanner, and array results were generated and initially analyzed using Illumina GenomeStudio Data Analysis Software (Illumina). The data were background corrected and listed by gene identification number for further analysis. Gene Set Enrichment Analysis (GSEA) and identification of differentially expressed genes was performed using the GSEA module of GenePattern, a freely available suite (http://www.broadinstitute.org/cancer/software/genepattern/) of genomic analysis software using the default settings. [15–17]

GSEA first calculates a ranked list of genes using a metric that reflects the correlation between the expression level of a gene and the class distinction between nanoparticle-treated and control samples. For each gene, we calculated the signal to noise score (S2N) metric, but results are not dependent on the choice of metric. $S2N=(\mu_{NP}-\mu_{BUFFER})/(\sigma_{NP}+\sigma_{BUFFER})$; μ_{NP} and σ_{NP} are the mean and standard deviation, respectively, of the expression level of the gene averaged across all AnxCLIO-Cy5.5 treated samples; μ_{BUFFER} and σ_{BUFFER} are the corresponding values across control treated samples. Given a pre-specified set of genes *S* (defined by a shared attribute, e.g. participating in the same biological pathway) GSEA asks if members of set *S* are randomly distributed throughout the ranked list, or are enriched at the top or bottom (as would be expected if members of set *S* can discriminate between nanoparticle treated and control cells). An enrichment score (ES) is calculated by walking down the ranked list of genes, and increasing a running-sum statistic whenever a member of set *S* is encountered, and decreasing the running-sum statistic whenever a gene that is not in set *S* is encountered. The enrichment score (ES) is defined as the greatest deviation from zero achieved by the running-sum statistic while walking through the entire ranked list; the ES is a weighted Kolmogorov-Smirnov-like statistic. Within GSEA, we utilized 1454 gene sets (http://www.broadinstitute.org/gsea/msigdb/collections.jsp#C5) based on Gene Ontology (GO) annotations of biological process, cellular component, and molecular function. We utilized the default filter to include only gene sets with between 15 and 500 members, which resulted in 731 sets being used in the final GSEA analysis. Asymptotic p-values and false discovery rates (FDR) were calculated within the GSEA module.

In Vivo Studies

Assessment of the impact of AnxCLIO-Cy5.5 on apoptotic cells in vivo was performed in a mouse model of myocardial ischemia-reperfusion. Transient ligation of the left coronary artery was performed in female wildtype C57BL6 mice (n=14) for 1 hour using a 7-0 nylon suture. The presence of myocardial ischemia was confirmed with continuous ECG monitoring, and core temperature was maintained above 37°C at all times. After 1 hour of ligation the suture was loosened, but left in place, and coronary flow was re-established. In half the mice (n=7), AnxCLIO-Cy5.5 (2mg Fe/kg body weight) was injected intravenously at the onset of reperfusion. Control animals (n=7) were injected with an equal volume of sterile PBS.

Echocardiography was performed in the mice prior to and 24 hours after ischemia-reperfusion. 2D and M-mode measurements of left ventricular function were made with a commercial ultrasound system (Vivid 7, GE Medical System, Milwaukee, WI) using a 13.0 MHz linear probe. The mice were lightly sedated with ketamine (16mg/kg body weight). LV end-diastolic (LVID) and systolic dimensions (LVIS) were measured on an M mode scan obtained in the parasternal short axis view at mid-papillary level. The left ventricular ejection fraction (EF) was calculated from the M Mode data $(LVID^3\text{-}LVIS^3)/LVID^3$. The cardiac output (CO) calculation method used a parasternal long axis 2 dimensional view. LV end-diastolic volume and LV end-systolic volume were calculated using a prolate-ellipsoid formula ($Volume=8A^2/3\pi L$, A=LV Area and L=LV length), and averaged on 5 consecutive cardiac cycles.

To assess changes in infarct size, mice were euthanized 24 hours after the onset of reperfusion. Immediately prior to euthanasia, repeat thoracotomy was performed and the suture that had been left in place around the left coronary artery was re-occluded. The presence of myocardial ischemia was confirmed with ECG monitoring. During coronary re-occlusion, the root of the aorta was clamped before 100μl of 10μm fluorescent microspheres (Invitrogen) were injected directly into the left ventricle and allowed to circulate via the coronary artery prior to euthanasia. The harvested hearts were cut in their short axis into 1mm thick sections with an automated tissue slicer (McIllwain Tissue Chopper, Vibratome, Bannockburn, IL), and soaked at 37°C in 1% triphenyltetrazolium chloride (TTC) for 10 minutes.

Following TTC staining, the harvested sections were fixed in 1% paraformaldehyde and imaged 24 hours later using a Nikon Eclipse TS100 fluorescent microscope (Nikon, Tokyo, Japan) to image the microspheres and a Leica MZ95 stereomicroscope (Leica, Solms, Germany) to image the TTC staining. The area-at-risk (AAR) was determined by the absence of fluorescent microspheres, and the presence of infarction by a lack of red staining with TTC. AAR and infarct size were traced manually by two experienced observers, who were both completely blinded to the type of injection the mice had received (AnxCLIO-Cy5.5 or PBS). Infarct size/AAR was calculated in the two groups and compared using an unpaired t-test (Prism). All studies and procedures were performed in accordance with the guidelines for the humane care of research animals at our institution, and were approved by the subcommittee on small animal research (SRAC) at our institution.

Results

A high degree of correlation was seen between the staining of apoptotic cells with Anx-FITC and AnxCLIO-Cy5.5 (Figure 1 A–B), confirming quantitatively the affinity of AnxCLIO-Cy5.5 for apoptotic cells. Time-lapse confocal microscopy of apoptotic cells exposed to AnxCLIO-Cy5.5 over a period of 7 hours showed that the probe remained bound to the outer cell membrane for approximately 3 hours, and was thereafter internalized by the cell (Figure 1C–D). Within 7 hours of exposure, AnxCLIO-Cy5.5 was no longer visible on the cell surface and was only seen as distinct punctate foci within the cell, presumably in endocytic vesicles.

AnxCLIO-Cy5.5 did not exert a deleterious effect on the energetics and metabolism of apoptotic cells. As expected, the JC-1 (mitochondrial membrane potential), Resazurin (reducing capacity), and CellTiter-Glo (ATP content) assays showed significant ($p<0.05$) changes between the apoptotic (CPT-exposed) and normal cells (Figure 2A–C). However, no differences in these energetics assays were seen between apoptotic cells that were exposed to AnxCLIO-Cy5.5 and those that were not.

The impact of AnxCLIO-Cy5.5 on cell membrane integrity was tested in rat myocyte (H9C2), human epithelial (786-0) and hamster ovarian cell lines (CHO). All lines showed a significant reduction in the number of early apoptotic cells becoming positive for propidium iodide (PI), when exposed to AnxCLIO-Cy5.5 (Figure 3A, 3B). However, no significant protective effect was seen when the cells were exposed to either Annexin V alone or to the unlabeled CLIO nanoparticle alone (Figure 3B). The protective effect produced by AnxCLIO-Cy5.5 was time dependent (Figure 3C) and reached statistical significance in those cells exposed to AnxCLIO-Cy5.5 for 7 hours. Caspase-3 activity in apoptotic cells exposed to AnxCLIO-Cy5.5 did not change significantly over time (Figure 3D).

A trend towards protection by AnxCLIO-Cy5.5 in vivo was also seen in the mouse model of myocardial ischemia-reperfusion. The two groups of mice (active group injected with

AnxCLIO-Cy5.5; control group injected with PBS) were well matched and no significant differences were seen in ejection fraction, cardiac output or area at risk (AAR) between the groups (Figure 4A–C). However, a trend ($p = 0.12$) towards a reduction in infarct size/AAR was seen in the mice injected with AnxCLIO-Cy5.5 (mean +/− SEM of 42.9 +/− 3.3% versus 51.2 +/− 3.7%, $p = 0.12$; or mean +/− SD of 42.9 +/− 8.7% versus 51.2 +/− 9.8 %; $p = 0.12$).

Gene expression analysis of early apoptotic cells exposed to AnxCLIO-Cy5.5 revealed that only a small number of genes showed significant changes (Figure 5). We performed Gene Set Enrichment Analysis to identify Gene Ontology (GO)-defined biological processes that were induced following AnxCLIO-Cy5.5 treatment. AnxCLIO-Cy5.5 caused upregulation of a limited number of gene sets related to amine, amino acid, and O-glycosyl bond hydrolysis, which may be due to intracellular metabolism of the nanoparticle's coating (consisting of cross-linked dextran with exposed amino groups). Conversely, gene sets related to ribosomes and RNA metabolism were downregulated following AnxCLIO-Cy5.5 treatment, which may be due to non-specific adsorption of ribosomal proteins to nanoparticles.[18] Importantly, gene sets associated with apoptosis, inflammation or response to oxidative stress were not significantly upregulated by exposure to AnxCLIO-Cy5.5 (Table 1).

Discussion

AnxCLIO-Cy5.5 is an apoptosis-sensing magnetofluorescent nanoparticle with considerable translational potential. The sensitivity and diagnostic power of the agent has been demonstrated in several preclinical studies. In the current study we show that AnxCLIO-Cy5.5 is well tolerated and has no deleterious effects on the apoptotic cells it binds to. In fact, exposure to AnxCLIO-Cy5.5 seems to exert a membrane-stabilizing protective effect on apoptotic cells in vitro, and possibly in vivo. These results further underscore the translational potential of AnxCLIO-Cy5.5 as a diagnostic nanoparticle, as a therapeutic, and as a vehicle for the delivery of novel therapeutics.

The AnxCLIO-Cy5.5 nanoparticle consists of Annexin V (Anx), cross-linked iron oxide (CLIO), and the near infrared fluorochrome Cy5.5. Annexin V is a 35 kD protein that has been used as a radiotracer in humans and has an extensive safety record.[5–7, 19] It is important to note that Annexin V is an endogenous protein produced by humans. Annexin levels in human plasma rise significantly in several disease states and a deficiency of annexin has been implicated in arterial thrombosis and autoimmune disease.[20] A strong biological basis thus exists to suggest that the injection of annexin at the dose needed in diagnostic or theranostic nanoparticles would be well tolerated.

The exposure of apoptotic cells to the CLIO nanoparticle alone did not influence membrane integrity. Likewise, the use of unmodified annexin V did not produce a protective effect. This suggests that larger annexin constructs (dimers, oligomers and nanoparticle constructs) are needed to enhance membrane stability. Annexin dimers (diannexins) are currently being investigated as therapeutic agents in the settings of arterial thrombosis and organ transplantation.[13] In addition to their size, these agents differ from unmodified annexin in that they exceed the renal threshold and have a long blood half-life. AnxCLIO-Cy5.5 likewise exceeds the renal threshold and has a blood half-life in mice of 2.7 hours.

Confocal microscopy in this study revealed that AnxCLIO-Cy5.5 remains on the surface of apoptotic cells for 3 to 4 hours, after which it is internalized. No changes in caspase-3 activity were seen in apoptotic cells exposed to AnxCLIO-Cy5.5. In addition, genomic analysis did not reveal changes in gene pathways likely to mediate cytoprotective effects.

We thus hypothesize that the protective effect of AnxCLIO-Cy5.5 is mediated via direct mechanical stabilization of the apoptotic cell membrane in a critical time window soon after injury. This is consistent with prior studies showing that annexin forms a complex lattice upon binding to the apoptotic cell membrane.[21, 22] The impact of this effect seems powerful enough to change the exponential rate constant of cell death and cause the kinetic (percent PI positive) curves of cells exposed and not exposed to AnxCLIO-Cy5.5 to continue to diverge.

The binding of unmodified Annexin V to phosphatidylserine on the surface of apoptotic cells has been well characterized.[23] In solution, Annexin V exists as a monomer. When bound to phosphatidylserine, however, Annexin V forms trimers with a convex surface facing the cell membrane.[21, 24] This leads to mechanical invagination of the membrane but conceivably could also buttress the cell membrane and attenuate outward bulging and rupture. Previous studies in lymphocytes have shown that Annexin V retards the development of cell death due to a membrane constraint effect.[14] We hypothesize that AnxCLIO-Cy5.5 exerts a similar effect on apoptotic cells. However, the aim of the present study was to characterize the safety of AnxCLIO-Cy5.5, and further study will be needed to elucidate the detailed mechanism and extent of its protective effect.

Magnetic iron-oxide nanoparticles (MNP) have been used clinically for almost 2 decades. When injected intravenously, untargeted MNP are taken up by the cells of the reticulo-endothelial system and are degraded over a period of 7 to 10 days.[25] The iron in the nanoparticle is metabolized much like endogenous iron, and is ultimately used to manufacture new red blood cells. Loading stems cells exogenously with very high concentrations of MNP has also been extensively studied and does not adversely affect their viability or metabolism.[26] The metabolism of targeted MNP, such as AnxCLIO-Cy5.5, is less fully defined. These agents are taken up by cells that do not have the extensive degradative capacity of the cells in the reticulo-endothelial system.[9, 25] Genome-wide gene expression analysis, however, did not reveal upregulation of gene sets related to inflammation, oxidative stress or apoptosis that would be consistent with AnxCLIO-Cy5.5 having a deleterious effect on the cell. These gene expression results are also consistent with recent data showing that labeling stem cells ex vivo with extremely high amounts of MNP did not produce any concerning changes in gene expression.[27]

The primary aim of this study was to determine whether AnxCLIO-Cy5.5 exerts a detrimental effect on apoptotic cells and accelerates their demise. This has been shown not to be the case. The suggestion in this study that AnxCLIO-Cy5.5 may actually be protective is an extremely interesting secondary result. The protective effect produced by AnxCLIO-Cy5.5 is smaller than reported with novel pharmaceuticals, such as caspase inhibitors. However, the production of even a small protective effect by a diagnostic imaging agent is noteworthy. It should also be noted that the translation of magnetic annexins into the clinical realm is highly feasible. Ferumoxytol (Advanced Magnetics, Lexington MA), a long circulating analogue of CLIO, was recently approved for clinical use and underscores the translational potential of AnxCLIO-Cy5.5. Annexin is a naturally occurring protein and has been extensively used in humans without safety concerns. Magnetofluorescent annexin constructs, analogous to AnxCLIO-Cy5.5, thus have the potential to become valuable diagnostic and theranostic nanoparticles in a broad range of clinical conditions.

Acknowledgments

We thank Michael Waring and Adam Chicoine for their assistance with cell sorting and Dr. Thomas Diefenbach for confocal microscopy.

Funding: Funded in part by R01 HL093038 (DES)

References

1. Whelan RS, Kaplinskiy V, Kitsis RN. Cell death in the pathogenesis of heart disease: mechanisms and significance. Annual review of physiology. 2010; 72:19–44.
2. Gottlieb RA, Burleson KO, Kloner RA, Babior BM, Engler RL. Reperfusion injury induces apoptosis in rabbit cardiomyocytes. The Journal of clinical investigation. 1994; 94(4):1621–1628. [PubMed: 7929838]
3. Korngold EC, Jaffer FA, Weissleder R, Sosnovik DE. Noninvasive imaging of apoptosis in cardiovascular disease. Heart failure reviews. 2008; 13(2):163–173. [PubMed: 18074226]
4. Dumont EA, Reutelingsperger CP, Smits JF, et al. Real-time imaging of apoptotic cell-membrane changes at the single-cell level in the beating murine heart. Nature medicine. 2001; 7(12):1352–1355.
5. Hofstra L, Liem IH, Dumont EA, et al. Visualisation of cell death in vivo in patients with acute myocardial infarction. Lancet. 2000; 356(9225):209–212. [PubMed: 10963199]
6. Kietselaer BL, Reutelingsperger CP, Boersma HH, et al. Noninvasive detection of programmed cell loss with 99mTc-labeled annexin A5 in heart failure. J Nucl Med. 2007; 48(4):562–567. [PubMed: 17401092]
7. Narula J, Acio ER, Narula N, et al. Annexin-V imaging for noninvasive detection of cardiac allograft rejection. Nature medicine. 2001; 7(12):1347–1352.
8. Sosnovik DE, Schellenberger EA, Nahrendorf M, et al. Magnetic resonance imaging of cardiomyocyte apoptosis with a novel magneto-optical nanoparticle. Magn Reson Med. 2005; 54(3):718–724. [PubMed: 16086367]
9. Chen HH, Josephson L, Sosnovik DE. Imaging of apoptosis in the heart with nanoparticle technology. Wiley interdisciplinary reviews. 2011; 3(1):86–99. [PubMed: 20945336]
10. Sosnovik DE, Garanger E, Aikawa E, et al. Molecular MRI of cardiomyocyte apoptosis with simultaneous delayed-enhancement MRI distinguishes apoptotic and necrotic myocytes in vivo: potential for midmyocardial salvage in acute ischemia. Circulation. 2009; 2(6):460–467. [PubMed: 19920044]
11. Sosnovik DE, Nahrendorf M, Panizzi P, et al. Molecular MRI detects low levels of cardiomyocyte apoptosis in a transgenic model of chronic heart failure. Circulation. 2009; 2(6):468–475. [PubMed: 19920045]
12. Shaw SY, Westly EC, Pittet MJ, Subramanian A, Schreiber SL, Weissleder R. Perturbational profiling of nanomaterial biologic activity. Proceedings of the National Academy of Sciences of the United States of America. 2008; 105(21):7387–7392. [PubMed: 18492802]
13. Teoh NC, Ito Y, Field J, et al. Diannexin, a novel annexin V homodimer, provides prolonged protection against hepatic ischemia-reperfusion injury in mice. Gastroenterology. 2007; 133(2): 632–646. [PubMed: 17681182]
14. Gidon-Jeangirard C, Hugel B, Holl V, et al. Annexin V delays apoptosis while exerting an external constraint preventing the release of CD4+ and PrPc+ membrane particles in a human T lymphocyte model. J Immunol. 1999; 162(10):5712–5718. [PubMed: 10229803]
15. Subramanian A, Tamayo P, Mootha VK, et al. Gene set enrichment analysis: a knowledge-based approach for interpreting genome-wide expression profiles. Proceedings of the National Academy of Sciences of the United States of America. 2005; 102(43):15545–15550. [PubMed: 16199517]
16. Mootha VK, Lindgren CM, Eriksson KF, et al. PGC-1alpha-responsive genes involved in oxidative phosphorylation are coordinately downregulated in human diabetes. Nature genetics. 2003; 34(3): 267–273. [PubMed: 12808457]
17. Reich M, Liefeld T, Gould J, Lerner J, Tamayo P, Mesirov JP. GenePattern 2.0. Nature genetics. 2006; 38(5):500–501. [PubMed: 16642009]
18. Park S, Hamad-Schifferli K. Enhancement of in vitro translation by gold nanoparticle--DNA conjugates. ACS nano. 2010; 4(5):2555–2560. [PubMed: 20384314]
19. Thimister PW, Hofstra L, Liem IH, et al. In vivo detection of cell death in the area at risk in acute myocardial infarction. J Nucl Med. 2003; 44(3):391–396. [PubMed: 12621005]
20. Blankenberg FG, Strauss HW. Will imaging of apoptosis play a role in clinical care? A tale of mice and men. Apoptosis. 2001; 6(1–2):117–123. [PubMed: 11321034]

21. Kenis H, van Genderen H, Bennaghmouch A, et al. Cell surface-expressed phosphatidylserine and annexin A5 open a novel portal of cell entry. The Journal of biological chemistry. 2004; 279(50): 52623–52629. [PubMed: 15381697]

22. Ungethum L, Kenis H, Nicolaes GA, Autin L, Stoilova-McPhie S, Reutelingsperger CP. Engineered annexin A5 variants with impaired cell entry for molecular imaging of apoptosis using pretargeting strategies. The Journal of biological chemistry. 2010

23. van Tilborg GA, Geelen T, Duimel H, et al. Internalization of annexin A5-functionalized iron oxide particles by apoptotic Jurkat cells. Contrast media & molecular imaging. 2009; 4(1):24–32. [PubMed: 19137542]

24. van Genderen HO, Kenis H, Hofstra L, Narula J, Reutelingsperger CP. Extracellular annexin A5: functions of phosphatidylserine-binding and two-dimensional crystallization. Biochimica et biophysica acta. 2008; 1783(6):953–963. [PubMed: 18334229]

25. Sosnovik DE, Nahrendorf M, Weissleder R. Magnetic nanoparticles for MR imaging: agents, techniques and cardiovascular applications. Basic research in cardiology. 2008; 103(2):122–130. [PubMed: 18324368]

26. Arbab AS, Bashaw LA, Miller BR, et al. Characterization of biophysical and metabolic properties of cells labeled with superparamagnetic iron oxide nanoparticles and transfection agent for cellular MR imaging. Radiology. 2003; 229(3):838–846. [PubMed: 14657318]

27. Kedziorek DA, Muja N, Walczak P, et al. Gene expression profiling reveals early cellular responses to intracellular magnetic labeling with superparamagnetic iron oxide nanoparticles. Magn Reson Med. 2010; 63(4):1031–1043. [PubMed: 20373404]

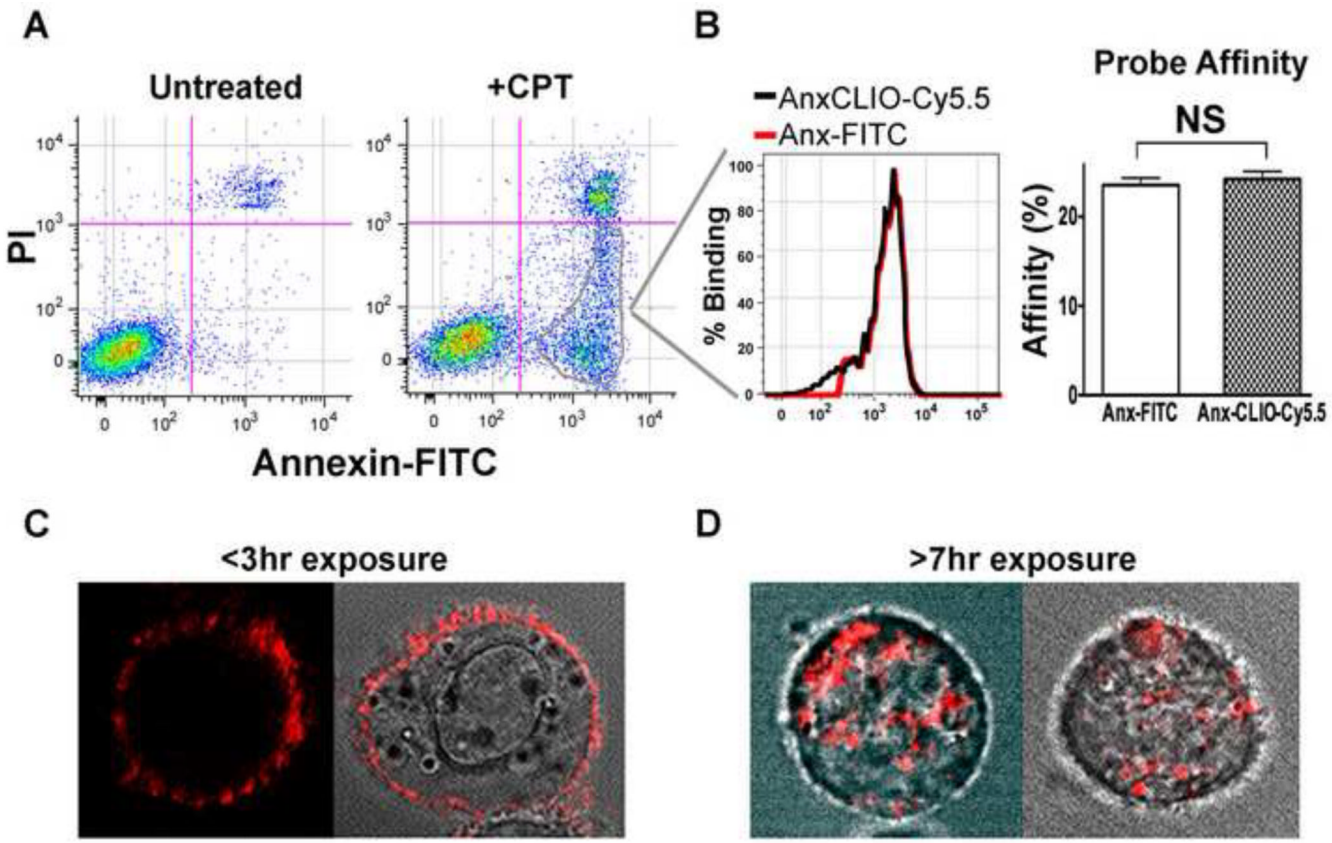

Figure 1.

Flow Cytometry and Confocal Microscopy of apoptotic cells exposed to AnxCLIO-Cy5.5. (A) Camptothecin (CPT) treatment induces three cell populations: normal (left lower quadrant), early apoptotic (right lower quadrant), and late apoptotic/necrotic (right upper quadrant). (B) The percentage of early apoptotic cells labeled with AnxCLIO-Cy5.5 is almost identical to the number labeled with Anx-FITC. Likewise, the percentage of total cells labeled with both probes is highly similar, suggesting that AnxCLIO-Cy5.5 has an equal affinity for apoptotic cells to that of Anx-FITC. (C, D) Time-lapse confocal microscopy of apoptotic 786-0 cells exposed to AnxCLIO-Cy5.5. (C) Three hours after exposure to the probe, AnxCLIO-Cy5.5 is exclusively visualized on the cell membrane. (D) Within seven hours of exposure, however, AnxCLIO-Cy5.5 has become completely internalized into the cells. Two sets of different cells are shown in each panel. NS=not significant ($p>0.05$).

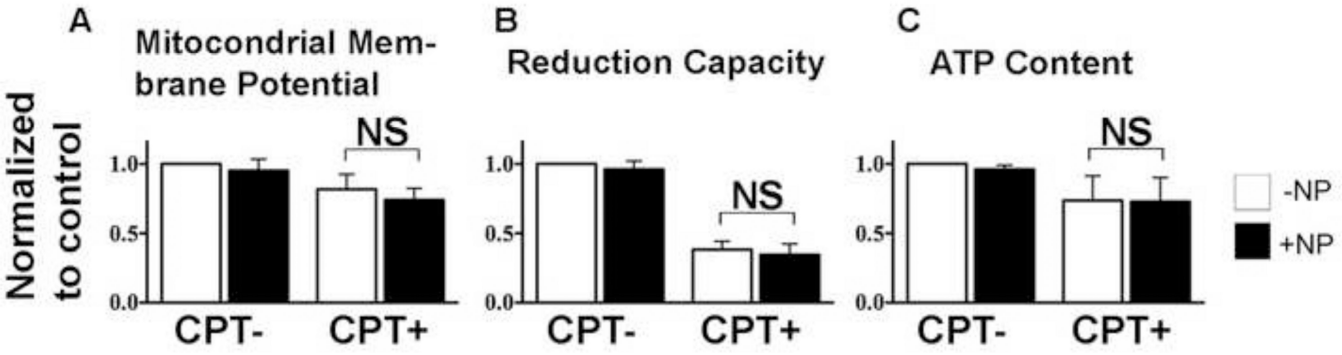

Figure 2.

Impact of AnxCLIO-Cy5.5 on cell energetics and metabolism. (A) Mitochondrial membrane potential (JC-1), (B) cell reduction capacity (Resazurin), and (C) cell ATP content (Celltiter Glo) assays show significant differences between camptothecin treated (CPT+) and normal cells. However, no differences are seen between apoptotic (CPT+) cells exposed to the AnxCLIO-Cy5.5 nanoparticle (+NP) or buffer only (−NP). AnxCLIO-C5.5 does not perturb the energetics or metabolism of apoptotic cells. NS=not significant ($p>0.05$).

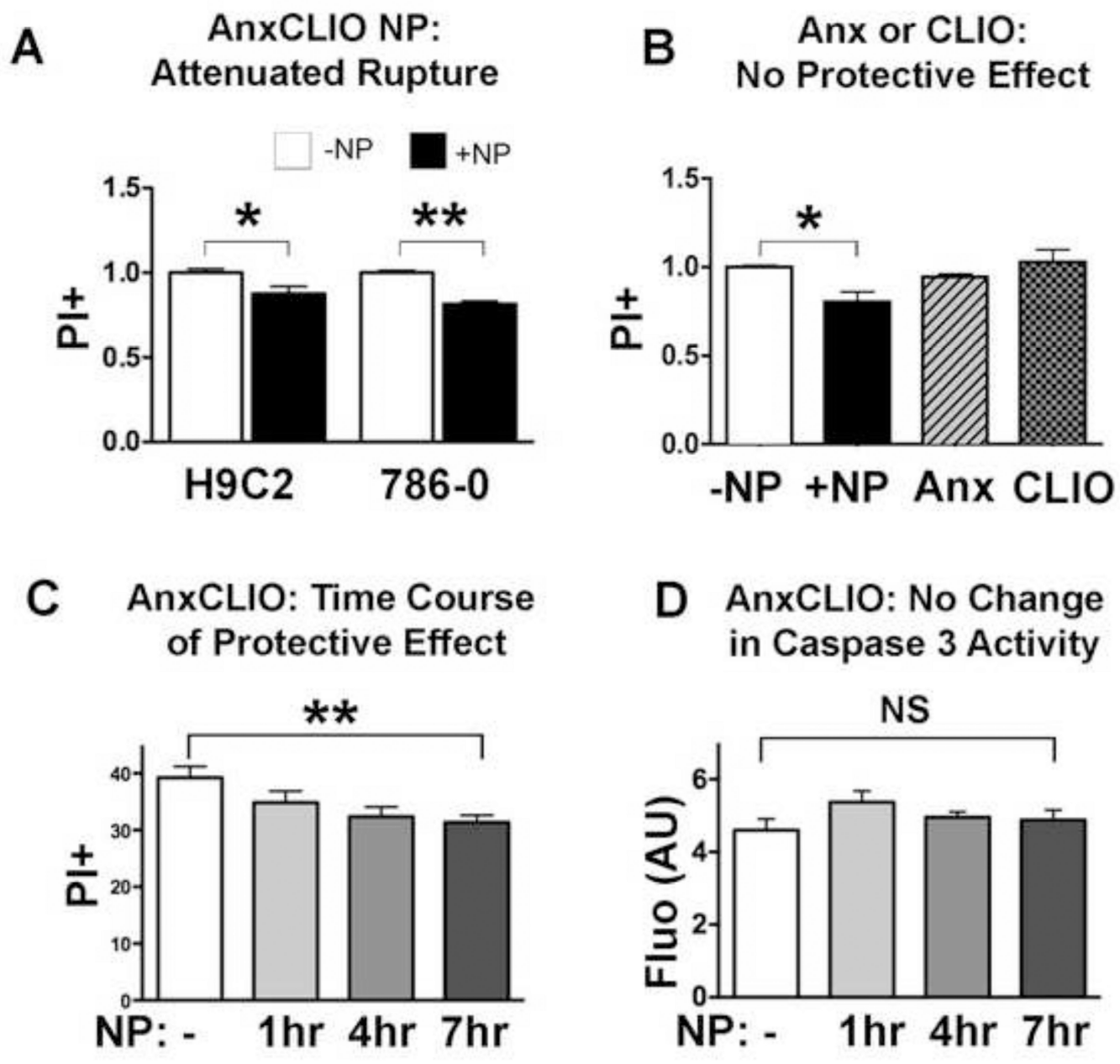

Figure 3.

Impact of AnxCLIO-Cy5.5 exposure on the membrane stability of early apoptotic (PI negative) cells. White bars = no nanoparticle, Black bars = AnxCLIO-Cy5.5 nanoparticle. (A) Exposure to the AnxCLIO-Cy5.5 nanoparticle (+NP), reduced the proportion of apoptotic cells undergoing membrane rupture and becoming PI positive. (B) Exposure of apoptotic CHO cells to either the AnxCLIO-Cy5.5 nanoparticle, annexin alone or the cross-linked iron oxide nanoparticle (CLIO). A protective effect was seen only with the annexin-labeled nanoparticle. No effect was seen with either annexin alone or the unlabeled nanoparticle alone. (C) The protective effect of AnxCLIO-Cy5.5 on membrane stability was greater in those batches of cells exposed to the probe for longer periods of time. (D) No significant differences in caspase-3 activity were seen in cells exposed to AnxCLIO-Cy5.5. This suggests that the protective effect of AnxCLIO-Cy5.5 is due to a direct effect on the

cell membrane and not on the apoptotic signaling cascade. *p<0.05; **p<0.01; NS=not significant (p>0.05).

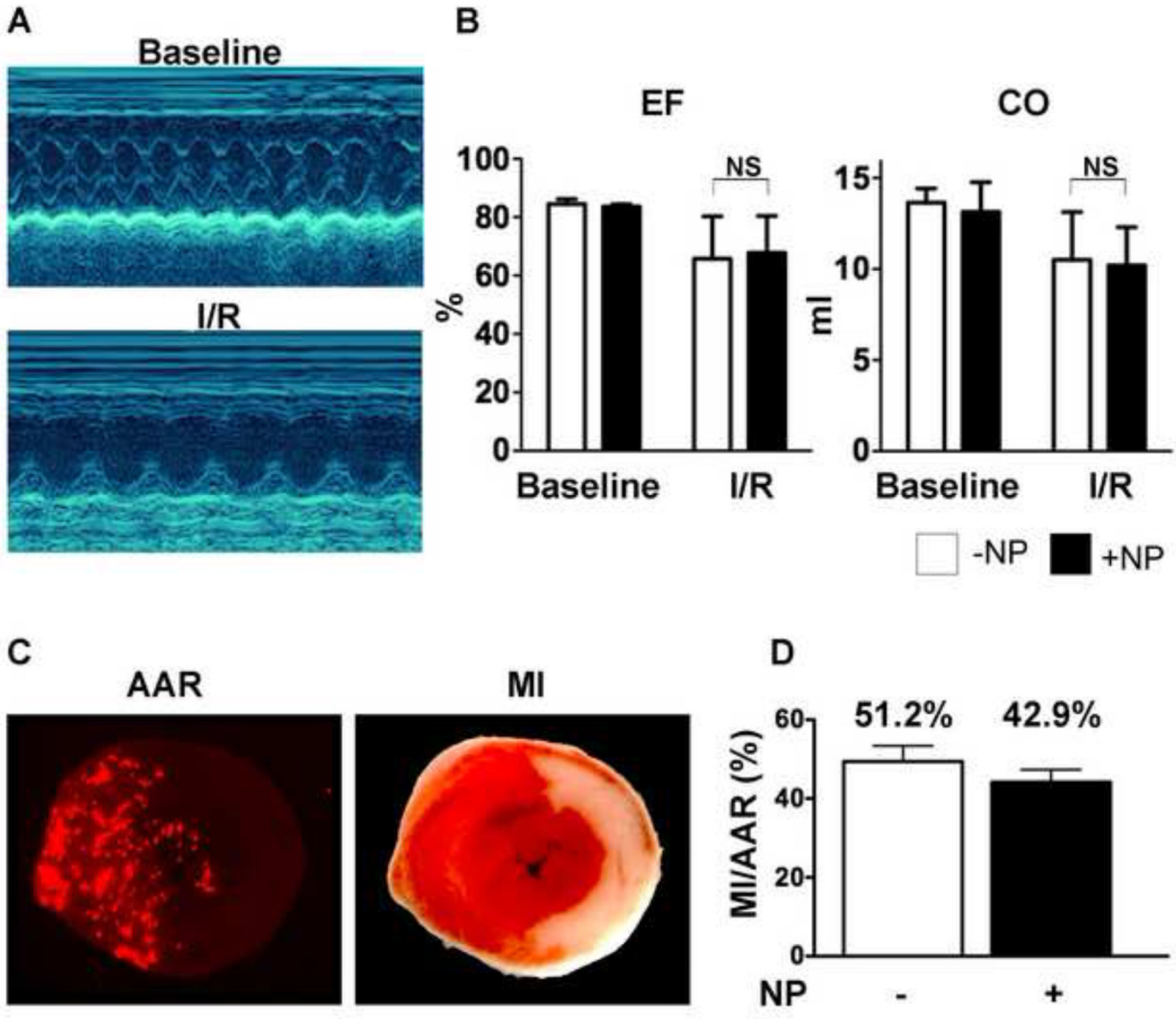

Figure 4.

Impact of AnxCLIO-Cy5.5 on mice exposed to ischemia-reperfusion injury (1 hour ligation of left coronary artery). The mice were injected intravenously at the onset of reperfusion with AnxCLIO-Cy5.5 (+NP) or PBS (−NP). (A) M-Mode echocardiography of a mouse heart before and 24 hours after surgery. The left ventricle is dilated and the anterior wall is severely hypocontractile 24 hours after surgery. (B) Ejection fraction (EF) and cardiac output (CO) were significantly lower after ischemia-reperfusion injury versus baseline, but there were no significant differences between those mice injected with AnxCLIO-Cy5.5 and PBS. (C) Measurement of infarct size (MI)/area at risk (AAR): The AAR in the section is defined by the absence of signal from fluorescent microspheres. The MI is defined by the pale area with TTC staining on the section. (D) MI/AAR was reduced by 16.2% in the mice injected with AnxCLIO-Cy5.5 (p=0.12).

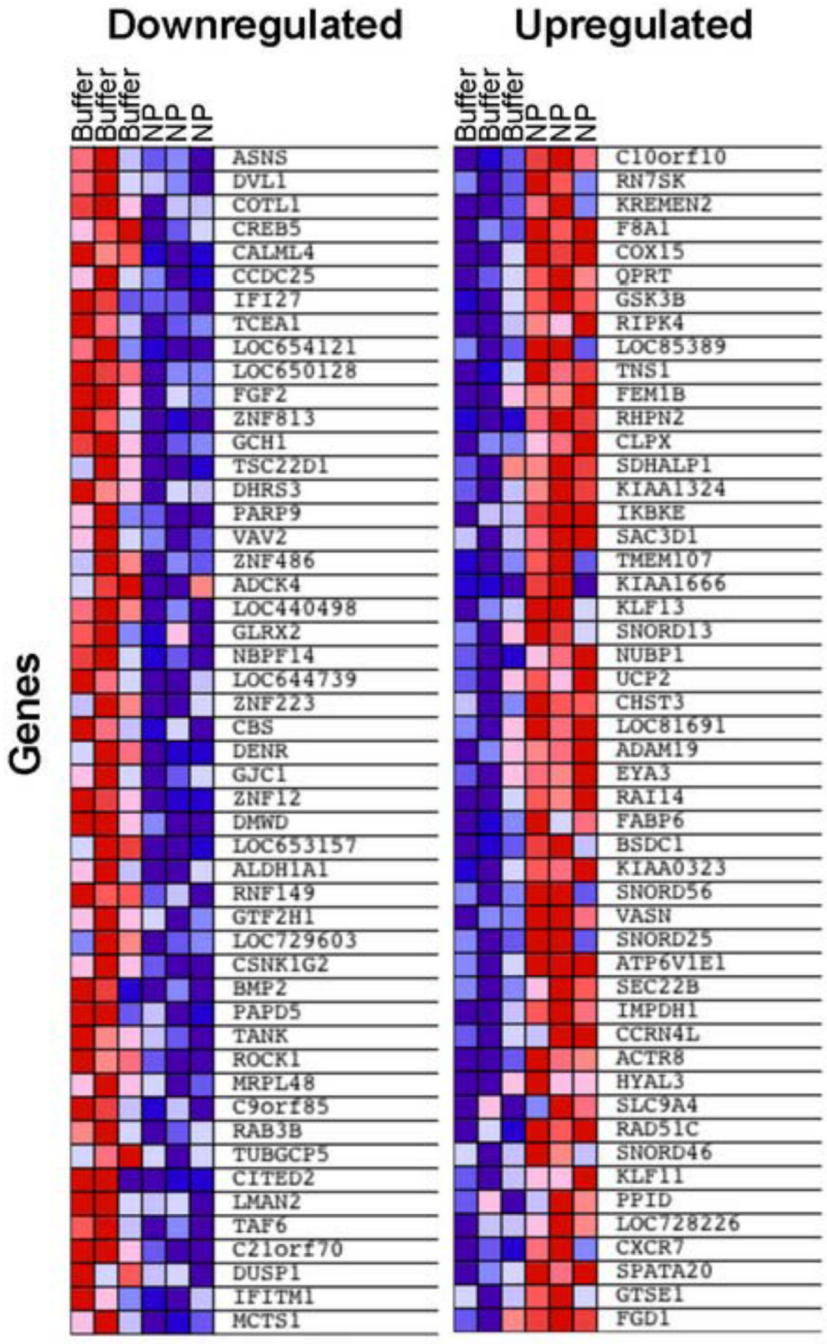

Figure 5.

Differentially expressed genes in apoptotic cells exposed to the AnxCLIO-Cy5.5 nanoparticle (NP) or buffer only. The most down- (left panel) and up-regulated (right panel) features (i.e. genes) in response to AnxCLIO-Cy5.5 (based on their signal-to-noise scores) are shown. Columns correspond to independent biological replicate samples. Heat map colors (red=high expression, blue=low expression) are normalized by row.

Table 1

Biological processes most affected in early apoptotic cells by exposure to AnxCLIO-Cy5.5, based on genome-wide gene expression and Gene Set Enrichment Analysis (GSEA). Top-ranking gene sets with p<0.05 and FDR (false discovery rate) <0.25 are shown. (A) Gene sets upregulated in AnxCLIO-Cy5.5 treated cells; (B) gene sets downregulated in AnxCLIO-Cy5.5 treated cells. ES=enrichment score; p=permutation p-value; FDR=false discovery rate.

A. Upregulated in AnxCLIO-Cy5.5-treated cells

Name	ES	p	FDR
AMINO_ACID_CATABOLIC_PROCESS	−0.66	<0.001	0.05
AMINE_CATABOLIC_PROCESS	−0.66	<0.001	0.06
AMINE_METABOLIC_PROCESS	−0.43	<0.001	0.07
CARBOHYDRATE_METABOLIC_PROCESS	−0.42	<0.001	0.08
NITROGEN_COMPOUND_CATABOLIC_PROCESS	−0.65	<0.001	0.08
ENZYME_INHIBITOR_ACTIVITY	−0.43	<0.001	0.17
MOTOR_ACTIVITY	−0.57	<0.001	0.18
HYDROLASE_ACTIVITY__HYDROLYZING_O_GLYCOSYL_COMPOUNDS	−0.56	<0.001	0.18
NITROGEN_COMPOUND_METABOLIC_PROCESS	−0.39	<0.001	0.19
CELLULAR_CARBOHYDRATE_METABOLIC_PROCESS	−0.39	<0.001	0.22

B. Downregulated in AnxCLIO-Cy5.5-treated cells

NAME	ES	p	FDR
EXTRACELLULAR_MATRIX_PART	0.54	<0.001	0.17
RRNA_PROCESSING	0.58	0.02	0.19
LOCOMOTORY_BEHAVIOR	0.49	<0.001	0.19
RNA_SPLICING__VIA_TRANSESTERIFICATION_	0.50	<0.001	0.20
RIBOSOME_BIOGENESIS_AND_ASSEMBLY	0.57	0.02	0.20
ANATOMICAL_STRUCTURE_FORMATION	0.52	0.01	0.22
RRNA_METABOLIC_PROCESS	0.58	0.02	0.22
GENERAL_RNA_POLYMERASE_II_TRANSCRIPTION_	0.52	0.01	0.23